New reactive polymer blends based on poly(urethane–ureas) (PUR) and polydisperse polydimethylsiloxane (PDMS): control of morphology using a PUR-*b*-PDMS block copolymer

Philippe Knaub, Yves Camberlin and Jean-François Gérard*
Laboratoire des Matériaux Macromoléculaires, UA CNRS No. 507, Institut National des Sciences Appliquées de Lyon, 20 Avenue A. Einstein, 69621 Villeurbanne Cedex, France
(*Received 23 October 1987; revised 17 February 1988; accepted 22 February 1988*)

After a study of the pure polydimethylsiloxane (PDMS) polydisperse network, blends of poly(urethane–ureas) (PUR) and PDMS were synthesized and characterized by means of differential scanning calorimetry, static and dynamic mechanical analysis, and scanning electron microscopy. All these techniques indicated total phase segregation between the two polymers, as a consequence of their great incompatibility. Between 10 and 40% PDMS, the PUR was in a continuous phase and the siloxane was dispersed in big non-adherent nodules (20–100 μm). The glass transition temperature (T_g) of the PDMS in these nodules is lower than the T_g of the pure PDMS. After phase inversion, little non-adherent PUR nodules (0.3–1 μm) were observed in a PDMS network. To compatibilize the two phases, small amounts of PUR-*b*-PDMS block copolymer were added. The resulting blends showed significant reduction in the PDMS dispersed nodule size and a dramatic increase in interfacial adhesion. As a consequence, the mechanical properties of the modified blends were enhanced. As is well known for incompatible thermoplastic blends, diblock copolymers with balanced composition are the most efficient interfacial agents. The best properties were obtained with only small amounts (0.5–2%) of copolymer, which corresponds to a good medium between the efficient interfacial activity of the copolymer and its plasticizing effect in a PUR matrix.

(Keywords: poly(urethane–ureas); polydimethylsiloxane; reactive polymer blend; morphology; mechanical properties)

INTRODUCTION

Recently, a number of studies have been performed on polyurethane-based interpenetrating polymer networks (IPNs) or, more generally, polymer blends[1–5]. IPNs are a class of blend where a polymeric network is synthesized in the presence of another previously or simultaneously established network[6]. The purpose of this work is to study blends of poly(urethane–ureas) (PUR) and polydimethylsiloxane (PDMS). The most important application of such blends is to obtain auto-withdrawing PUR materials, which could then be employed for both casting and RIM processes. The surface tension of PDMS is very low[7,8], in the range $(1.9–2.1) \times 10^{-2}$ N m^{-1}.

A few studies have been performed on PUR–PDMS[2] or on PDMS-based polyurethanes (instead of polyether or polyester soft phase)[9,10], and the authors always found almost total segregation between the phases. In the case of a blend, macro-segregation is observed. As the term IPN implies interpenetration of the two polymer networks held together by permanent entanglements, we cannot use it in our case, so a term like 'interstitial composites', used by Koberstein[11] for instance, is more appropriate.

In this study the poly(urethane–ureas) used are linear block copolymers based on poly(tetramethylene oxide) (PTMO), aliphatic diisocyanates and aromatic diamines. For reviews of PUR synthesis, characterization and properties, see a preceding publication[12]. The PDMS used are two-part liquid silicone rubbers (Dow Corning) called Silastic LSR. Details of the structure and properties of these elastomers are given in the first part of this study.

For the blends, two PUR systems are chosen: the first is based on a 2000 molecular-weight soft segment, whereas the second is synthesized with a 1000 molecular-weight PTMO. The isocyanates and diamines are also changed to retain the same reaction kinetics in the two systems.

The synthesis of the blends was very difficult owing to the great incompatibility of the original materials, so it was decided to introduce an emulsifier in small amounts as the third component. These compatibilizing agents were polyether–PDMS block copolymers. Such AB copolymers are well known to provide stabilization against gross segregation upon processing and to improve adhesion[13–15]. However, all the studies on this subject have been carried out on thermoplastic homopolymers.

EXPERIMENTAL

Synthesis

The polyurethane synthesis has been described in preceding work; for details see ref. 12.

Silicone rubbers

Two liquid silicone rubbers were tested in this study:

---

* To whom correspondence should be addressed

0032–3861/88/081365–13$03.00

Silastic LSR 595 and LSR 599 (Dow Corning). Silastic A and B are two-part silicone elastomers supplied as A and B components specifically designed for liquid injection moulding. Significant product features of Silastic A and B liquid silicone rubbers include (Dow Corning specifications): (a) 1:1 mixing ratio; (b) long pot life; (c) rapid cure rate; and (d) high viscosity of the A and B components (1000–8000 P).

Mixing and vulcanization of the PDMS

The A and B components were mixed in a laboratory kneader (IKA HKD 0.6) at room temperature for 10 min. Even mixing is assured due to the intensive action of the broad-bladed kneaders. The two components are moved around the trough in both vertical and horizontal directions. The kneaders interact deeply and narrowly and are driven by a geared motor that has a torque overload device[16]. The PDMS is then poured into a mould and pressed for a given time at a temperature higher than 100°C.

PUR–PDMS blends

A polyurethane prepolymer (based on one mole of PTMO and three moles of diisocyanates) and a one-to-one ratio of Silastic A and B were carefully mixed in a glass reactor for 15 min under vacuum at 60°C. The polyurethane chain extender (aromatic diamine) was then added. After 20 s of very strong mixing, the blend was cast into a mould at 120°C and cured for 3 h at this temperature.

The experimental process was always kept rigorously the same; this is very important because the speed of mixing certainly influences the final morphology of the blends.

Characterization

Gel permeation chromatography. A Waters chromatograph was used with tetrahydrofuran (THF) solvent for the PUR analysis and toluene for the PDMS ones, and using Microstyragel columns with 1000, 500, 100 and 100 Å pore size. Detection was achieved by differential refractometry. The product concentration was 2 mg ml^{-1} and the flow rate 1.5 ml min^{-1}.

Nuclear magnetic resonance. N.m.r. spectra were obtained from solution in C_6D_6 at 350 MHz with a Cameca 350 apparatus.

*Fourier transform infra-red spectroscopy. FT*i.r. spectra were obtained using a Nicolet model MX1 with a DTGS detector. All spectra were obtained using 2 cm^{-1} resolution in the standard 1 min measurement mode. Liquid samples were placed between two KBr windows and the solid ones were mixed in small amounts with KBr powder and then pressed into discs.

Differential scanning calorimetry. A Mettler TA 3000 microcalorimeter was used for heat-capacity measurements in argon, with heating rates of 7.5 K min^{-1}. A cooling rate of 10 K min^{-1} was used from room temperature to −170°C with a sample weight of about 15 mg. Scanning from −170°C provides excellent baselines for ΔC_p measurements.

Dynamic mechanical measurements. Dynamic mechanical data were collected at 11 Hz using a Toyo–Baldwin Rheovibron DDV IIB viscoelastometer with a heating rate of 2°C min^{-1}.

Static mechanical measurements. Stress–strain properties were measured on a DY25 Adamel Lhomargy testing apparatus at room temperature with a crosshead speed of 5 or 25 mm min^{-1}, respectively, for determinations of the elasticity modulus and the ultimate properties.

The elongations of the samples were determined by an LVDT contacting extensometer, which provides a very good resolution (10 μm accuracy measured with a strength gauge). Samples were cut with an NFT 51-034 H2 die and had a gauge length of 25 mm.

Gel-point measurements. These kinetics were performed on a Rheomat 115. The gel time was determined as the tangent of the viscosity *versus* time curve when the viscosity increases dramatically.

Scanning electron microscopy. The morphology of the blends was investigated by scanning electron microscopy. Fracture surfaces were prepared at either −90°C (environmental test chamber of a flexural testing apparatus) or liquid-nitrogen temperature (Charpy pendulum impact tester) and observed by SEM (JEOL JSM T200).

Swelling of the networks. Swelling ratios q, defined as the ratio of the volume of the swollen film to that of the unswollen one, were obtained in benzene, cyclohexane and 2-butanone (methyl ethyl ketone, MEK). A sample of each PDMS film, approximately 3 cm square and 0.1 cm thick, was weighed and then placed in the solvent in covered Petri dishes at room temperature. They were removed every day, blotted dry with absorbent tissue as carefully and quickly as possible, and reweighed (in fact, the weight loss of the strips is measured as a function of time and the swelling weight at $t=0$ obtained by extrapolation).

The swelling equilibrium was reached between one and a few days. The extent of swelling was characterized by v_{2m}, the volume fraction of the (already extracted) polymer at equilibrium (maximum) swelling. It was calculated by assuming simple additivity of volumes.

RESULTS AND DISCUSSION

Preliminary study of the PDMS networks

Physicochemical characterization of the A and B components. The Silastic PDMS are industrial rubbers, so chemical analyses were necessary to determine the structure and functionality of the A and B components.

*Fourier transform infra-red spectroscopy. FT*i.r. spectroscopy was used to determine the backbone of the rubbers and also the functional groups. A typical spectrum is shown in *Figure 1*. We find in it the characteristic bands of polysiloxanes[17]: (a) The Si–O–Si band gives rise to one very intense band in the 1100–1000 cm^{-1} region owing to the antisymmetric stretching mode. (b) A band at 1258 cm^{-1} is exhibited by our products and is due to the symmetric methyl deformation $Si–CH_3$. (c) $Si–(CH_3)_2$ groups are also present and the samples show absorption in the 800 cm^{-1} region. (d) A C=C stretching vibration (from the Si–vinyl groups) lies at 1595 cm^{-1} for the A and B samples. (e) An intense Si–H stretching vibration occurs at 2164 cm^{-1} for the B samples only. The last two bands are characteristic of the functional groups.

In order to follow the disappearance of the hydride and vinyl bands during crosslinking, *FT*i.r. spectra have been recorded at 120°C. In the first few minutes the peaks rapidly reduce, but after this time the change becomes very small, and it is not possible to remove the two peaks entirely. So one can see that never all the functions do not react.

In order to corroborate these results, an n.m.r. study of the A and B samples has been performed.

^1H nuclear magnetic resonance study. The n.m.r. spectra of 595A and 595B are shown in *Figure 2*. These spectra confirm the *FT*i.r. results. Indeed, one can observe the Si–CH_3 resonance near 0.1 ppm on the two spectra. The other small peaks represent side-chain reactive groups. A multiplet is observed for the two samples in the 5.6–6.3 ppm area and is attributed to the Si–CH=CH_2 group[18,19]. The SiH resonance is observed only on the 595B spectrum near 4.7 ppm. These results all confirm the *FT*i.r. study.

It is also possible to obtain a quantitative evaluation of the average molecular weight between two vinyl or two hydride functions by measuring the relative intensity of the vinyl or hydride peak with regard to the O–Si–CH_3 one. (The data of the area under the peaks are obtained by computation.) One can see in *Table 1* the results obtained for the 595 and 599 samples. It is not possible to infer the average molecular weight between crosslinks $\bar{M}_c$ of the networks because the distribution of the hydride and vinyl functions along the chains and the chain lengths are unknown. Nevertheless, *Table 1* gives the average molecular weights between two hydride or two vinyl functions. The A and B components are mixed in a one-to-one ratio, so one can see that the stoichiometry is not exact. Indeed, there is a large excess of hydride functions (2–2.5 times more SiH groups than vinyl ones, but the accuracy of the measurements is rather poor).

A similar case has been studied by Mark[20,21]: an $Si(OSi(CH_3)_2H)_4$ crosslinking agent was reacted with vinyl groups along PDMS chains and the reaction mixture contained two moles of SiH per mole of Si–CH=CH_2, since using one-half the stoichiometric quantity of SiH should give crosslinks having an average functionality of 4.

In our case, it is not possible to find out if, in the B component, the vinyl and hydride groups are on the same chains or if there are chains with only vinyl substitutions (like the A component) plus short PDMS chains with a few (four and more) hydride functions[22].

Gel permeation chromatography. Analyses were carried out by g.p.c. with toluene as solvent. One can observe (*Figure 3*) a high polydispersity of both A and B components. On the 595 curves the distribution is more regular than on the 599 ones, which show a bimodal distribution in the area of high molecular weights. A difference is also observed between the A and B components in the 400–4000 molecular-weight area (polystyrene equivalents). Otherwise the four chromatographs have the same profile and the same molecular weight at the start of the curve.

The molecular weights are collected in *Table 2*. On the basis of Lapp *et al.*'s work[23], which compared PDMS molecular weights obtained by g.p.c. in toluene with three different calibrations, we calculated an absolute PDMS molecular weight (using PDMS secondary standards and Lapp's data). These last weights are just an approximation, and with such a high polydispersity it is not possible to compare them with the n.m.r. data. The

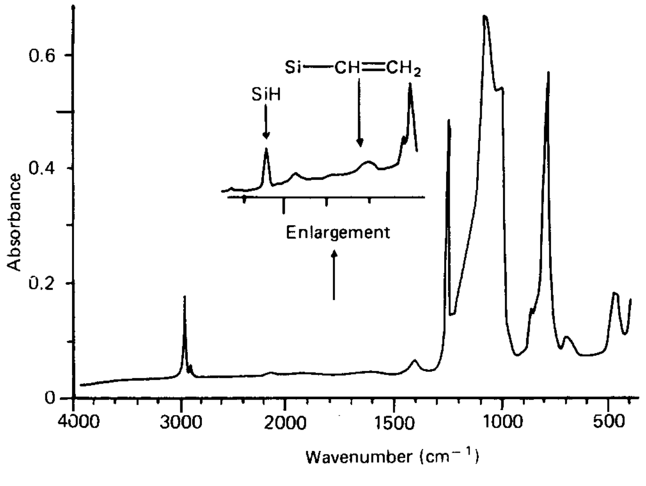

Figure 1 *FT*i.r. spectrum of Silastic 595B

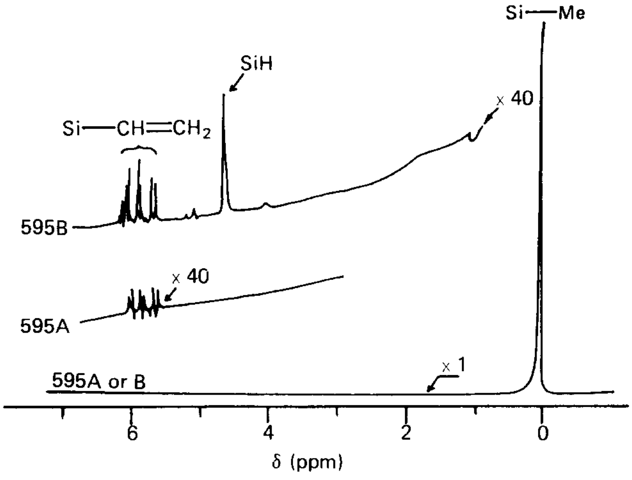

Figure 2 N.m.r. spectra of Silastic 595A and 595B

Table 1 N.m.r. study of PDMS elastomers: quantitative determination of the molecular weight between hydride or vinyl functions

Sample	Number of –$OSi(CH_3)_2$ groups	Number of SiH functions	Number of vinyl functions	Molecular weight between SiH groups (g)	Molecular weight between vinyl groups (g)
595A	one (6 protons)	–	0.00526	–	14 700
595B	one (6 protons)	0.0244	0.00526	3030	14 700
599A	one (6 protons)	–	0.00666	–	11 110
599B	one (6 protons)	0.0322	0.00666	2300	11 110

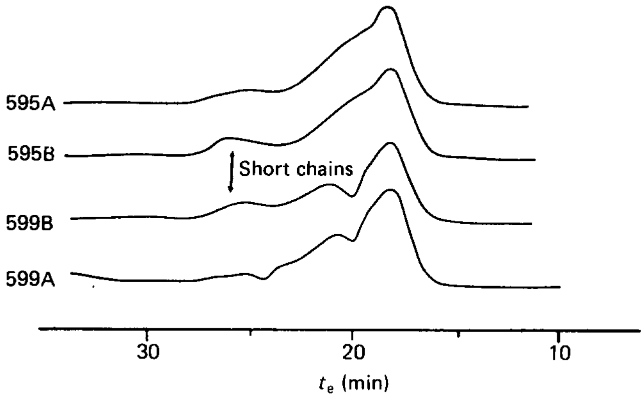

Figure 3 G.p.c. chromatograms of Silastic components

Table 2 Molecular weights of the Silastic obtained by g.p.c.

	Polystyrene calibration			PDMS calibration		
Sample	M_n (g)	M_w (g)	I_{poly}	M_n (g)	M_w (g)	I_{poly}
595A	9 100	92 300	10.3	8 200	83 000	10.1
595B	6 200	92 400	14.8	5 600	83 200	14.8
599A	11 800	96 200	8.1	10 600	86 600	8.2
599B	7 200	94 600	13.1	6 500	85 100	13.1

difference observed between the A and B components is perhaps due to short PDMS chains with hydride reactive groups, as in the assumption mentioned above.

Differential scanning calorimetry measurements. All the four products (595A, 595B, 599A and 599B) exhibit a low glass transition temperature (−127°C), a crystallization peak near −95°C and a double melting peak (−55°C), as observed by other workers[24]. After reaction of A and B and curing for 3 h at 120°C, the glass transition temperature of the network is still the same (−127°C), a crystallization peak occurs at −105°C and a single melting peak at −62°C. The exothermicity of the reaction is very weak, about 7.2 J g^{-1}.

Dynamic mechanical properties. The curves are shown in *Figure 4*. They have typically elastomeric profiles. The rubbery plateau begins near −20°C and the modulus increases when the temperature rises; this is readily explained by the almost entropic nature of rubber elasticity[25]. The modulus normally varies as the absolute temperature over all the temperature range of the rubbery plateau.

The modulus of the 595 samples is lower than that of the 599 one, as predicted by the n.m.r. data (higher molecular weights between both two hydride and two vinyl functions for the 595 sample).

The simplest but universally used expression relating the modulus to the molecular weight between crosslinks is[26–28]:

$$E=3g(\rho/\bar{M}_c)RT$$

where g is the front factor, ρ is the density of the network, $\bar{M}_c$ is the average molecular weight between crosslinks, R is the universal gas constant and T is the absolute temperature. The term $\rho/\bar{M}_c$ represents the number of chains per unit volume, and g is a factor varying from 0 to 1, which depends mainly on the functionality of the network (factor $(\phi-2)/\phi$)[29,30] and on the non-affineness of the displacements. We make the assumption that, for very small deformations, the behaviour is affine. So the value of the front factor is very close to $2(\phi-2/\phi)$. We must now determine ϕ. The unbalanced hydride–vinyl stoichiometry has been pointed out by both *FT*i.r. and n.m.r. analyses. A few authors[31,32] attribute this excess of hydride functions to secondary reactions. Very recent investigations on the side reactions of hydrosilation[32] reported that approximately 30% of the SiH groups are lost. Of this, 2 to 3% react with moisture and the remaining part, as much as 28%, is consumed in diverse redistribution reactions. So with a tetrafunctional crosslinking agent, only three of the four functions react and the average functionality of the junctions of the network becomes $\phi=3$. So $g=1/3$ and

$$\bar{M}_c=\rho RT/E$$

Under these conditions, we find ($T=293$ K; $\rho=1120$ kg m^{-3}):

$$\bar{M}_{c,595}=2500\text{ g} \qquad \bar{M}_{c,599}=1250\text{ g}$$

Swelling measurements. To corroborate the $\bar{M}_c$ values, equilibrium swelling measurements were carried out on each of the network strips, in benzene, cyclohexane and 2-butanone (MEK) at room temperature. The swelling results are summarized in *Table 3*. The most reliable interpretation of the swelling results utilizes the recent theory of Flory[33]. In the theory, the extent to which the deformation is non-affine depends on the looseness with which the crosslinks are embedded in the network

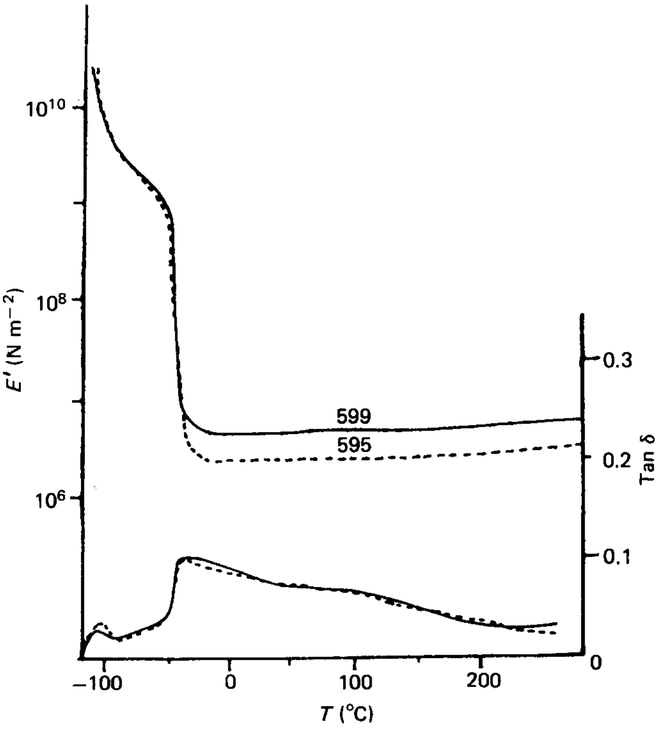

Figure 4 Dynamic mechanical curves of Silastic components

Table 3 Swelling data of the Silastic components

Samples	q	v_{2m}	v_{2c}	$V_1{}^a$ ($cm^3 g^{-1}$)	χ_1	χ_1+K	M_c (g)
595 in MEK	2.16	0.462	0.963	90.1	0.688	1.29	2950
595 in cyclohexane	3.66	0.273	0.962	108.7	0.479	1.37	3550
595 in benzene	2.87	0.347	0.963	89.4	0.597	1.34	4200
599 in benzene	2.56	0.391	0.963	89.4	0.612	1.32	2250

[a] From ref. 35

structure. The relation used by Mark *et al.* is:

$$\bar{M}_c = \frac{-\rho V_1 2c^{2/3} v_{2m}^{1/3}(1+K)/2}{\ln(1-v_{2m}) + v_{2m} + \chi_1 v_{2m}^2}$$

in which v_{2c} is the volume fraction of polymer incorporated in the network structure ($1-v_{2c}$ is obtained by extraction), v_{2m} is the volume fraction of polymer in the network at swelling equilibrium ($v_{2m}=1/q$), ρ is the density of the unswollen network, $(1+K)$ is a factor characterizing the extent to which the deformation in swelling approaches the affine limit, V_1 is the molar volume of the solvent and χ_1 is the free energy of interaction between the solvent and the PDMS network. Flory and Takara[34] showed that χ_1 was also dependent on the swelling ratio and found the expression:

$$\chi_1 = 0.481 + 0.335 v_{2m}$$

for the benzene–PDMS system at 25°C. Two similar expressions can be found in the literature for two other systems (at 25°C):

$$\chi_1 = 0.48 + 0.45 v_{2m}$$

for PDMS–MEK[35]

$$\chi_1 = 0.43 + 0.18 v_{2m}$$

for PDMS–cyclohexane[36].

The quantity K is a function not only of v_{2m} but also of two network parameters, k and p, which specify, respectively, the constraints on the crosslinks from neighbouring chains and the dependence of the crosslink fluctuations on the strain. For PDMS networks, reasonable estimates of these parameters are $p=2$ and $k=20$[29–31]. Values of $(1+K)$ could then be obtained by interpolation of Flory's plots of this factor *versus* v_{2m}. These values are given in the sixth column of *Table 3*. One can see great differences between the results of $\bar{M}_c$ when the solvent is changed. The value obtained with 2-butanone (MEK) as swelling agent underestimates the real value because MEK is a θ solvent for PDMS at 20°C[37], and hence a bad one at 25°C (the swelling ratio q is very small). The other two solvents are good ones for this system, but nevertheless 15% divergence between the two $\bar{M}_c$ data is observed, which can be explained by the experimental errors and by the choice of the various parameters required for the $\bar{M}_c$ calculation.

Yet, the comparison between the 595 and 599 $\bar{M}_c$ values is interesting and the results are not too far from the data obtained from the plateau modulus (with the non-affine behaviour assumption).

Stress–strain measurements. (The stresses were always measured after equilibrium.) Stress–strain isotherms were plotted using the semi-empirical equation of Mooney and Rivlin[38] but no linear behaviour could be observed over a large range of strain. At room temperature, PDMS networks are amorphous without strain-induced crystallization[39]. Mark *et al.*[40] studied PDMS with bimodal chain length distribution and found such behaviour. The increase in modulus should demonstrate non-Gaussian effects due to the limited chain extensibility of the short chains[30,32]. This could corroborate the assumption of hydride reactive groups on short silicone chains (see g.p.c. results).

Conclusion of the preliminary study

This study showed how it was possible to characterize a PDMS network with the classical analytical techniques. We just used the theory of rubber-like elasticity as a tool and did not try to elaborate on or support such a theory, or to find out if the permanently trapped entanglements[41,42] do or do not have a great influence on the final properties of the network. The study reveals the following:

(a) The A component is composed of PDMS chains with vinyl reactive groups (*FT*i.r., n.m.r) and probably a tin- or platinum-based catalyst[43].

(b) The B component is composed of PDMS chains with vinyl reactive groups (*FT*i.r., n.m.r) and hydride substituents, perhaps short chains (g.p.c.)[32], in an approximately 1:3 total stoichiometric excess of hydride functions.

(c) The network non-linear behaviour on the Mooney–Rivlin plots could be interpreted as a consequence of a non-Gaussian distribution of chain lengths and so could corroborate the g.p.c. results.

(d) The $\bar{M}_c$ of the networks has been studied by two methods: first at very small deformations (E' measurements) with the assumption of non-affine behaviour and secondly by swelling measurements with Mark and Flory's data and theory.

The correlation between the two methods is reasonable.

Study of the PUR–PDMS blends

On the basis of this preliminary work, we have synthesized blends based on these PDMS networks and on the PUR studied in an earlier work[12]. We chose to keep the same PDMS network 595 in the whole study, but to use two PUR systems having the same reactivity. The first one (called PU1) is based on one mole of poly(tetramethylene oxide) (PTMO) with a molecular weight of 2000 as soft phase, three moles of trimethylhexamethylene diisocyanate (TMDI) and two moles of methylene-*bis*-2-methyl-6-ethylaniline (MMEA) as chain extender. The second one (called PU2) is composed of one mole of PTMO (with a molecular weight of 1000), three moles of isophorone diisocyanate (IPDI) and two moles of methylene-*bis*-2,6-diisopropylaniline. The first system based on PTMO 2000 is quite viscous at 60°C, and the second one is more fluid, facilitating the process.

Gel-point measurements of the polyurethane systems. The mixing temperature has been adjusted to give approximately the same gel point in the two systems. This is an essential parameter because it controls the final morphology of the blend. The first system reaches the gel point after 2 min (approximately) at 55°C and the second one after 2.5 min at 65°C. These temperatures are then kept the same in the whole study.

Study as a function of the PUR–PDMS ratio. The sample designation code indicates whether the PUR is based on 1000 or 2000 PTMO and the percentage of PDMS of the sample. For example, PUR 1000–20–595 indicates a blend of 80% PTMO 1000-based poly(urethane–ureas) and 20% PDMS 595. The entire range of blends have been synthesized with the two PUR systems.

Kinetics of polymerization of PUR and PDMS. The rate of the reactions is obtained by two methods: first by viscosity measurement, giving the gel points of the systems, and secondly by d.s.c. isotherm measurements, which give the exothermicity of the reactions. The results are plotted in *Figure 5*. The different components are mixed at 55 or 65°C (see Experimental), then quickly poured into a mould and cured for 3 h at 120°C. So the beginning of the reaction occurs at low temperature and the end at 120°C. One can see that the polyurethane system reacts more quickly than the PDMS, so it will mainly form before the siloxane network. This observation is very important in understanding the morphology of the blends. The discrepancies observed between the d.s.c. and viscosity data can easily be explained: In one case (d.s.c.), we measure principally the beginning of the reaction, when the number of reactions is important and the exothermicity is high. In the other case, the viscosity measurements give the gel point (infinite viscosity), characterizing more complete reaction.

FTi.r. spectroscopy. FTi.r. spectroscopy was used to check that the two reactions were almost complete, by following the disappearance of the NCO stretching band (located near 2270 cm^{-1}) for the PUR system and the diminution of the SiH band. For all the blends, the conversion of PUR is greater than 95%, but not accurately detectable for PDMS.

D.s.c. analysis. Figure 6 shows d.s.c. thermograms of pure siloxane 595, pure PU1 and two blends, PUR 2000–20–595 and PUR 2000–80–595; the blends and polyurethane samples were quenched into liquid nitrogen before the run. One can see that, for the blends, two glass transitions and two melting peaks are clearly observed (corresponding respectively to PDMS and PTMO).

The main d.s.c. results are summarized in *Table 4*. It should be observed that the accuracy of some data is quite mediocre when the PTMO or PDMS of the blend is in small amounts.

The incompatibility of the two systems is very great and the blends reflect the superposition of the two networks: the glass transition and heat-capacity changes of PTMO in pure polyurethane and in the blends are unchanged. The same observations can be made with the ΔC_p of PDMS; the glass transition of PDMS is even lower for the

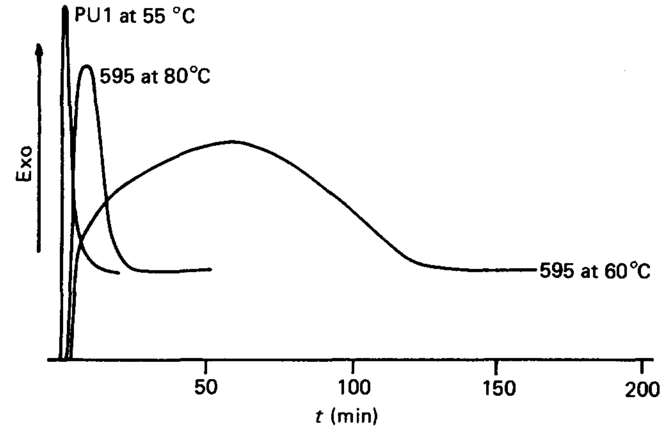

Figure 5 Heat of reaction of PUR and PDMS measured by d.s.c.

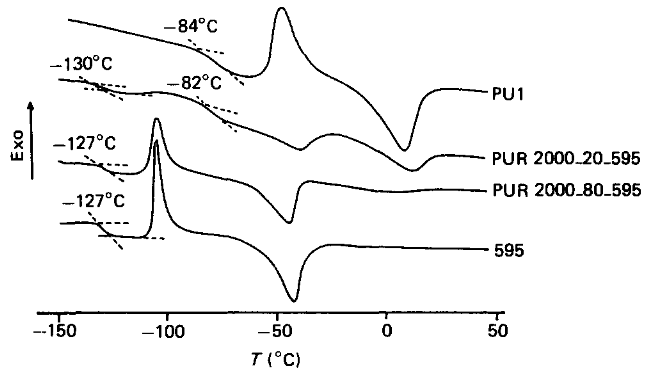

Figure 6 D.s.c. thermograms of PUR–PDMS blends

Table 4 D.s.c. data for the blends and pure PU1 and Silastic 595

Sample	PU1	PUR 2000 –10–595	PUR 2000 –20–595	PUR 2000 –30–595	PUR 2000 –40–595	PUR 2000 –50–595	PUR 2000 –60–595	PUR 2000 –70–595	PUR 2000 –80–595	PUR 2000 –90–595	595
PDMS											
ΔC_p (J g^{-1} K^{-1})	–	(0.44)	(0.40)	0.43	0.40	0.40	0.41	0.38	0.38	0.39	0.40
T_g (°C)	–	−132	−132	−132	−129	−128	−127	−127	−128	−127	−127
PTMO											
ΔC_p (J g^{-1} K^{-1})	0.51	0.51	0.52								–
T_g (°C)	−84	−84	−83	−82	−83	−82	−83	U[a]	U[a]	U[a]	–

[a] Undetectable

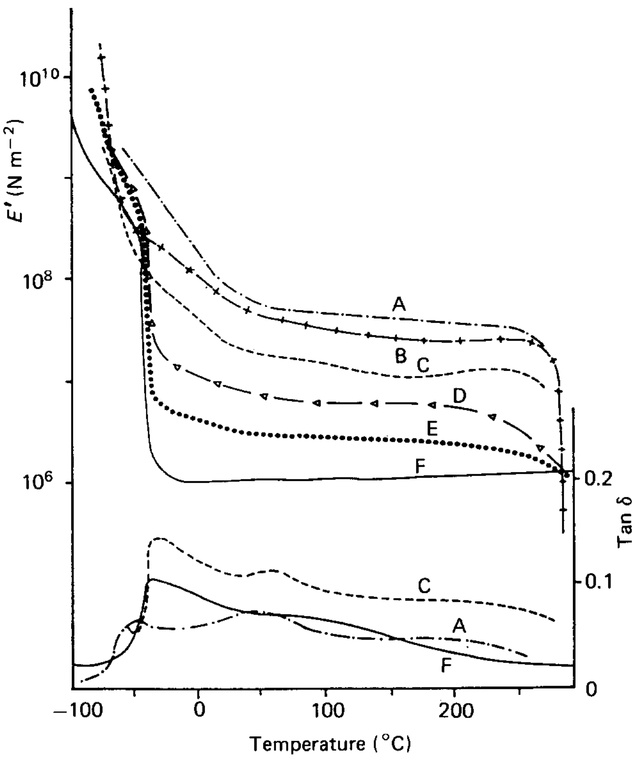

Figure 7 Dynamic mechanical properties of PU1-based blends: PU1 (curve A); PUR 2000–20–595 (curve B); PUR 2000–40–595 (curve C); PUR 2000–60–595 (curve D); PUR 2000–80–595 (curve E); and 595 (curve F)

blends than for pure PDMS. This last point will be discussed later in view of other results.

Dynamical mechanical measurements. The curves are plotted in *Figures 7* and *8*, where tan δ data indicate three or four maxima for the blend samples occurring at approximately −100°C, −60°C, −40°C and +20°C. The low-temperature loss peak (−100°C) is attributed to the backbone motion of PDMS chains that accompanies its glass transition, whereas the −40°C loss peak is related to fusion of the crystalline part of the PDMS network (see the preliminary study). The other two peaks are related to polyurethane: the low-temperature loss peak (−60°C) is characteristic of the soft-segment glass transition and the high-temperature one (+20°C) corresponds to fusion of the crystalline part of the PTMO segments (see ref. 12). These results are in good agreement with those obtained by d.s.c. For the blends rich in PDMS, one can see two rubbery plateaux on the E' curves: the first normally occurs around 0°C and ends at 240°C, and the second appears at 270°C; the end of this latter plateau is not detectable with our apparatus. The first plateau corresponds to the PDMS network reinforced with PUR inclusions; these nodules are damaged when the temperature rises above 250°C[12], so the storage modulus decreases up to the pure PDMS network plateau (brought back to the volume fraction of PDMS). One can see a phase inversion occurring around 50% PDMS; before phase inversion we have a PUR matrix with PDMS inclusions, and after phase inversion the opposite situation obtains.

Figure 9 shows the change of the storage modulus (E') *versus* the volume percentage of PDMS in the blend; it is obvious that phase inversion occurs near the inflection point of this curve. The profile of the curve can be predicted simply by Takayanagi's models: his parallel model for the mechanical behaviour of a two-component system[44] corresponds to the case in which the stiffer component (poly(urethane–ureas)) is continuous, while his series model corresponds to the case in which the softer component (PDMS) is continuous. The left of the curve in *Figure 9* clearly agrees with the parallel model (between 0 and 30% PDMS), while between 70 and 100% PDMS the series model is better.

To corroborate the displacement of the glass transition of the PDMS observed by d.s.c. (see *Table 4*), viscoelastic measurements have been carried out with a PL/DMTA from Polymer Laboratories at 3 Hz. Scanning from −160°C provides excellent baselines for tan δ; it is thus possible to measure accurately the beginning and the maximum of the PDMS loss peak (the temperature is given to ±1°C). Unfortunately, this peak occurs in the same area as the transition of the PTMO, which appears to involve local motions in the PTMO chains[26–45]. So, for the blends, it is not possible to detect the beginning of

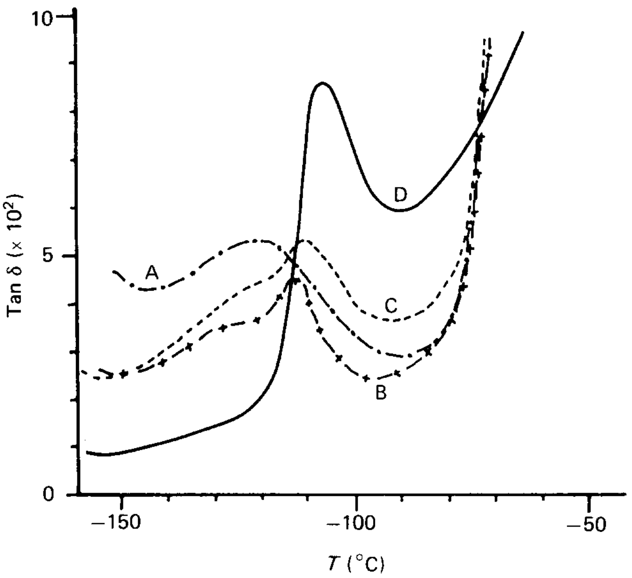

Figure 8 Low-temperature loss peak of some blends measured by p.l./d.m.t.a.: PUR1 (curve A); PUR 2000–10–595 (curve B); PUR 2000–30–595 (curve C); and PDMS 595 (curve D)

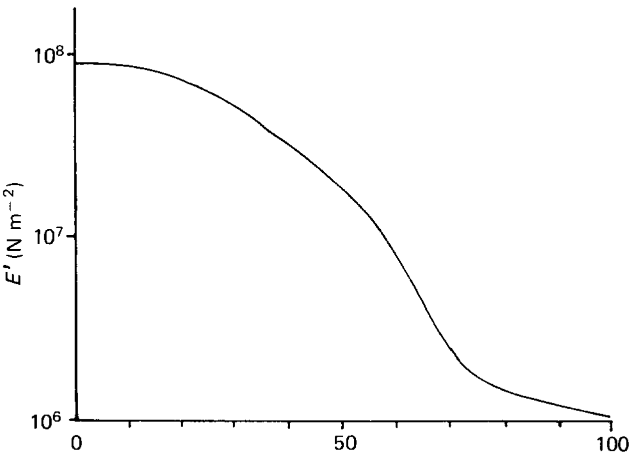

Figure 9 Evolution of the storage modulus (E') *versus* the percentage (in volume) of PDMS in the blend

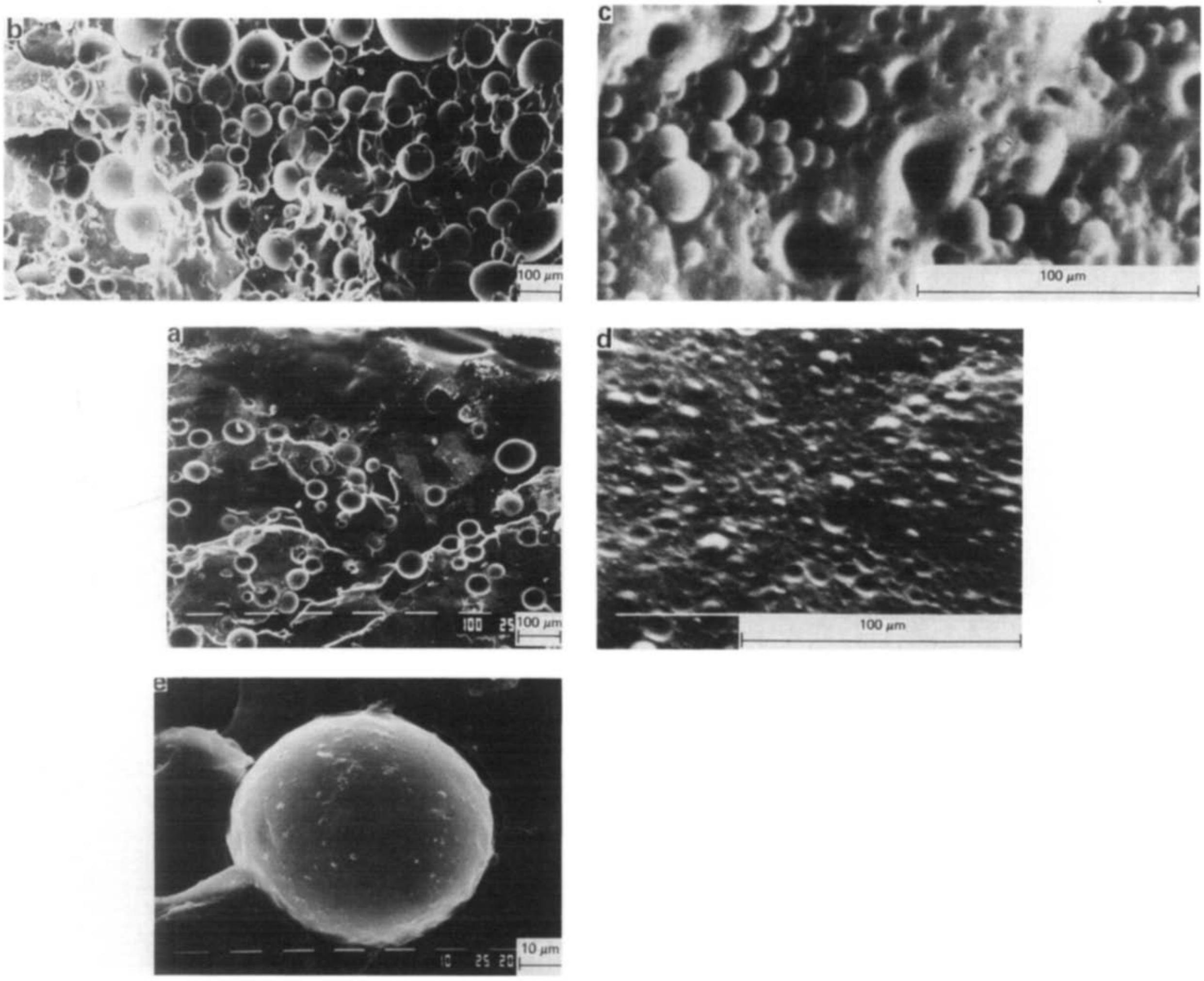

Figure 10 Scanning electron micrographs of (a) and (e) PUR 1000–10–595; (b) PUR 1000–40–595; (c) PUR 1000–60–595; and (d) PUR6 1000–90–595

the peak (see *Figure 8*). Nevertheless, one can see significant differences between the maximum temperatures of the peaks: −106°C for pure PDMS, −110°C for the blend with 30% PDMS and −113°C for the blend with 10% PDMS, confirming the trend observed by d.s.c. To explain these results, a morphological study seems to be necessary.

Scanning electron microscopy. The morphology of PUR–PDMS blends was thoroughly investigated by means of SEM in order to report the influence of the ratio of PDMS on the final structure. The same trend is observed for the two PUR systems; an example of four PTMO 1000-based blends is shown in *Figure 10*. On the micrographs *10a* and *10b*, the matrix is polyurethane and the nodules are composed of PDMS. After phase inversion (*10c* and *10d*) the continuous phase is polysiloxane and the PUR is dispersed. The great incompatibility of the two systems is reflected by the non-adhesion of the nodules (see micrograph *10e*). The sizes of the nodules of the dispersed phase are summarized in *Table 5*. The data are the result of a few hundred measurements for each sample. The (debatable) assumption is made that the real diameter of the nodules is the one observed (as adhesion is non-existent between the two phases, this hypothesis is taken to be true). One can see in *Table 5* that phase inversion occurs between 40 and 50% PDMS. The particle sizes and particle size distributions normally increase when the concentration of the separated phase increases. The great difference between the PUR and PDMS nodule sizes can easily be explained by differences in the speed of reaction and viscosity of the two systems: In one case, the polyurethane, dispersed in a viscous PDMS matrix, first reacts and gives small PUR nodules; in the second case, the viscous PDMS is dispersed in a fluid PUR matrix, which reacts quickly and gels the structure of big unreacted PDMS nodules.

In view of all these results, we can try to interpret the decrease in the glass transition of the PDMS network in the blend. A few theories have been proposed in the literature. Unfortunately, any one of them could be utilized in our case.

The size of the nodules of PDMS is too important to explain the change in the glass transition. Indeed, in a study performed in our laboratory[5], it has been shown that, in the case of interpenetrating networks of poly(urethane–ureas) and polyacrylate, the nodules of PTMO obtained had a size as small as 100 Å, but their glass transition nevertheless occurred at the same temperature as when the polyether was in a continuous phase.

Table 5 Particle sizes and particle size distributions (μm) of the dispersed phase, measured from SEM micrographs

PUR 1000 –10–595	PUR 1000 –20–595	PUR 1000 –30–595	PUR 1000 –40–595	PUR 1000 –50–595	PUR 1000 –60–595	PUR 1000 –70–595	PUR 1000 –80–595	PUR 1000 –80–595
52 ± 12	55 ± 21	85 ± 35	91 ± 50	0.9 ± 0.35	1.05 ± 0.95	0.73 ± 0.45	0.57 ± 0.23	0.28 ± 0.14

The decrease in tan δ_{max} temperature could also be interpreted by an increase in molecular weight between crosslinks in the nodules (compared to that in the PDMS continuous phase). But in the case of PDMS chains the Si–O–Si group is so mobile that no glass transition could be observed even between unreacted chains and the PDMS network. Indeed, the molecular weight between crosslinks is too high in these systems to show any difference.

The representation and interpretation of dynamic mechanical properties of polymer–polymer composites were discussed by Dickie[46] in terms of equivalent mechanical models and the viscoelastic form of the well known Kerner equation. Unfortunately, at least one of the assumptions made by Dickie is not valid in our work. The adhesion between matrix and inclusions is not perfect: it is taken to be non-existent. Nevertheless, our experimental observations (decrease in the glass transition temperature of the inclusions) and Dickie's are identical.

Another phenomenological explanation is readily proposed: after 3 h curing at 120°C, the sample is cooled to room temperature, so the difference in thermal expansion coefficients between the PDMS and PUR networks can generate free volume and so decrease the glass transition temperature. Thermal expansion coefficients were determined with the Mettler thermomechanical analyser (TMA); in the 30–120°C temperature range we found:

$$\alpha_{PDMS} = 3.1 \times 10^{-4}\,°C^{-1}$$

$$\alpha_{PUR2000} = 1.9 \times 10^{-4}\,°C^{-1}$$

So α_{PDMS} is greater than $\alpha_{PUR2000}$ as required for the present explanation. Two points make this assumption unacceptable. First, to create a depression and free volume in the PDMS nodules, good adhesion between the phases is needed and, as we showed, this is not the case here. Secondly, the shrinkage that occurs during polymerization must be taken into consideration. The shrinkage due to isocyanate–amine condensation is quite important (around 0.8 %) when that due to hydride–vinyl polyaddition is very small. So it is obvious that this shrinkage would widely compensate for the difference in thermal expansion.

So, at this moment, no reasonable explanation of this glass transition temperature decrease can be proposed. Indeed, all the explanations mentioned above are unacceptable for at least one reason (generally the non-adhesion between the PUR matrix and the PDMS inclusions).

Study of the (PUR–PDMS) modified blends

In order to stabilize the blends and control the morphology, diblock copolymers were added in small amounts. This method is now commonly used to enhance the compatibility of thermoplastic blends (polystyrene–polyethylene and polystyrene–poly(methyl methacrylate), for example)[15,47–49]. It is clear that adding an AB copolymer to a simple mixture of A and B homopolymers enhances the compatibility but cannot improve the miscibility of the homopolymer mixture[50]. The use of block copolymers as non-anionic detergents and as oil-in-oil emulsifiers are examples of the development of such materials. The immiscibility of PUR and PDMS promotes the (desired) segregation of phases but is also responsible for the high interfacial tension and poor adhesion between the phases. This prevents the achievement of a fine dispersion and promotes the gross segregation observed in the preceding part of this paper. The lack of interfacial adhesion is also a barrier to efficient transfer of stress between the phases and explains the weak mechanical properties observed. So enhancement in the degree of compatibility between the homopolymers seems necessary and can be sought by addition of a third component that reduces the number of unfavourable contacts between segments of the two polymers. It has been shown that under certain conditions the spinodal, the binodal and the critical temperatures of the ternary mixtures are expected to decrease linearly with the amount of copolymer added[15,48,49]. In this work, two blends have been studied with different amounts of copolymer: PUR 2000–30–595 and PUR 1000–30–595. The choice and synthesis of the emulsifier are now described.

Nature and synthesis of the copolymer. As mentioned before, the emulsifier was chosen to be a polyurethane-*block*-PDMS copolymer. Several workers[13,14,32] have noted that the compatibilizing effect in bulk mixtures is greater when the homopolymers are of lower (or comparable) molecular weight than the blocks in the block copolymer. Unfortunately, it was not possible to find a telechelic amine-terminated PDMS of molecular weight higher than 3000 (aminopropyl-terminated polydimethylsiloxane, PS 510 from Petrarch), approximately half the average molecular weight between crosslinks of the PDMS network. The urethane block is composed of poly(propylene oxide) (with 6% ethylene oxide) monoamine (Jeffamine M2005 from Texaco) with molecular weight 2000, which is miscible with PTMO. To link these two PDMS and polyether chains and form urea groups, an isophorone diisocyanate (IPDI) has been used in a two-step reaction at −40°C, as at room temperature the speed of the reaction between aliphatic amine and isocyanate is too high. Another advantage of working at low temperature is that the difference in reactivity of the two isocyanate functions of IPDI increases when the temperature decreases[51–53]; so it may be possible to react the aliphatic isocyanate preferentially, as it is more reactive than the cycloaliphatic one.

The reactions are followed by g.p.c. with THF as solvent. In the first step M2005 and IPDI are mixed in a one-to-one ratio at −40°C for a few hours. The temperature is then raised to 20°C in order to be sure that the reaction is complete. The g.p.c. chromatogram of this first step reaction is shown in *Figure 11*. The larger peak represents molecules formed by MP2005 reacted with IPDI; the other peak (higher weights) is attributed to M2005–IPDI–M2005 molecules; so a little excess of IPDI is of course observed.

The second step of the reaction consists of adding half a mole of PDMS (difunctional) to a mole of the prepolymer synthesized in the first step (monofunctional). The process is the same as in the first step and we obtain a final viscous product with (number) average molecular weight of 7400 and a quite small polydispersity of 1.70.

The process for the modified blends is the same as for the non-modified ones; the copolymer is added at the beginning of mixing in amounts between 0.5 and 10% (by weight).

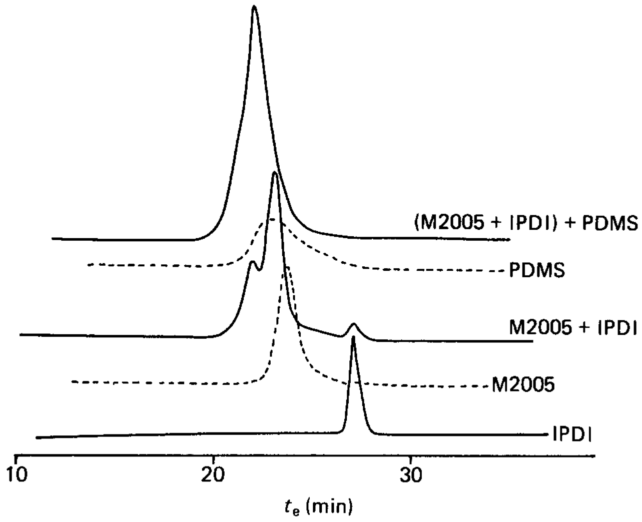

Figure 11 G.p.c. chromatograms of the PUR-*block*-PDMS reactions

D.s.c. analysis. No significant differences can be observed between the modified and unmodified blends; the same glass transition temperatures were measured.

Dynamic mechanical analysis. The curves are shown in *Figures 12a* and *12b*. The same trend is observed for the two groups of curves: for low amounts of copolymer (0.5% and 1%) the modulus is the highest, and for higher ones (5% and 10%) the modulus becomes inferior to that of the unmodified blend. All the curves are more or less parallel, showing no high-temperature enhanced behaviour with the copolymer. The storage moduli (E') measured with the Rheovibron are not accurate enough to show correctly the differences between the blends; static mechanical measurements were therefore undertaken.

Stress–strain measurements. The Young's moduli and elongations at break are summarized in the first two lines of *Table 6*. The results show the same trends as the dynamic mechanical data. More precisely, with 5 or 10% copolymer the mechanical behaviour of the blends is worse. In this case the copolymer acts more like a plasticizer and its interfacial activity is displaced by the excess of emulsifier. For the 0.5%, 1% and 2% samples the results are better than for the unmodified blend, especially for the elongation at break. These results will be explained on the basis of the morphology of the blends.

SEM observations. SEM micrographs of PUR 1000–30–595 modified blends are shown in *Figure 13*. One can see the great influence of the amount of emulsifier added to the blend. The size of the nodules and their adhesion to the matrix are both dramatically changed with quite small amounts of copolymer (between 0.5 and 2%). The same trend is observed with PUR 2000-based blends, as shown in *Figure 14*.

For the PUR 2000-based blend with 5% modifier, no nodules could be observed. just a kind of small steps very difficult to observe by microscopy. The sizes and distribution of the modified blends are given in the third

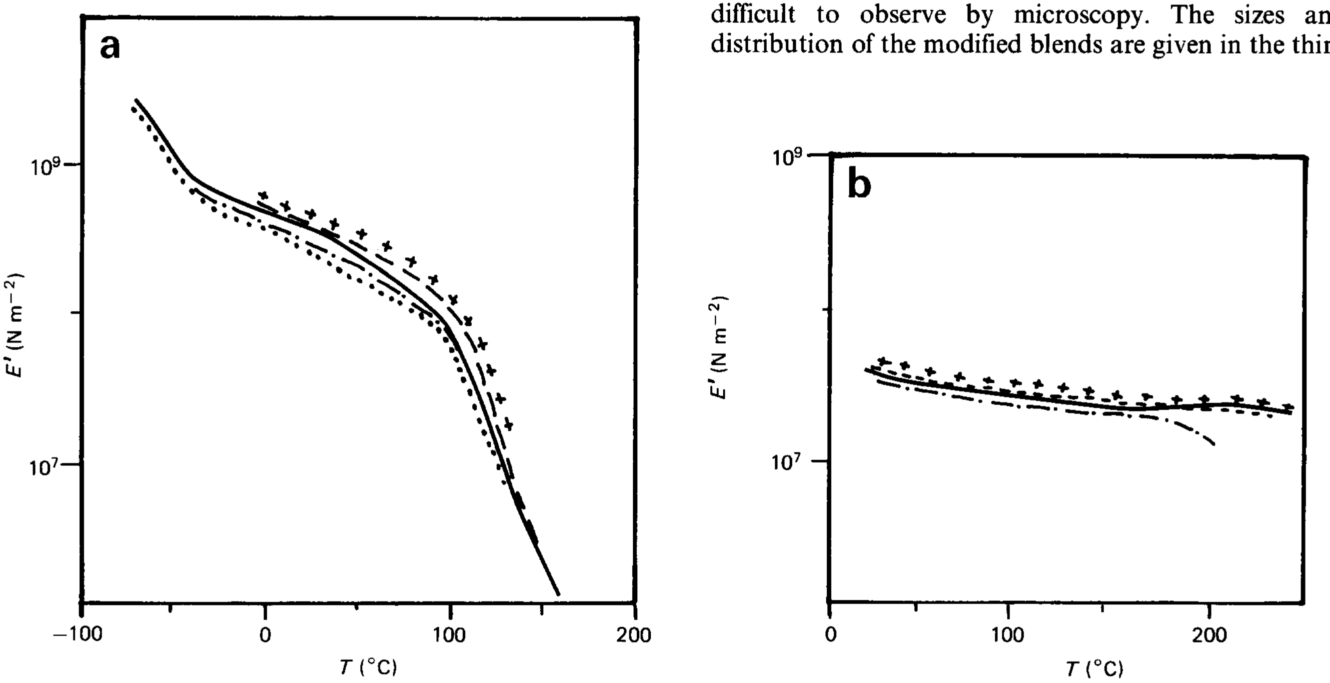

Figure 12 Dynamic mechanical curves of (a) PUR 1000–30–595 and (b) PUR 2000–30–595 with different amounts of copolymers: 0% (———); 0.5% (- - - - -); 1% (+ + +); 5% (–·–·–); and 10% (·····)

Table 6 Tensile data and particle size measurements for the modified blends

	PUR 2000–30–595					PUR 1000–30–595					
	0%[a]	0.5%	1%	2%	5%	0%[a]	0.5%	1%	2%	5%	10%
E (MPa)	41±2	41±2	43±3	36±3	30±2	400±10	420±30	590±30	400±30	330±50	310±50
ε_r (%)	390±30	500±30	470±30	460±60	320±30	170±10	210±10	210±10	215±10	150±10	160±10
Particle size (μm)	19±8	11±4	8±3	4.9±2	–	85±35	32±11	31±20	24±9	22±10	12±7

[a] Percentage of copolymer

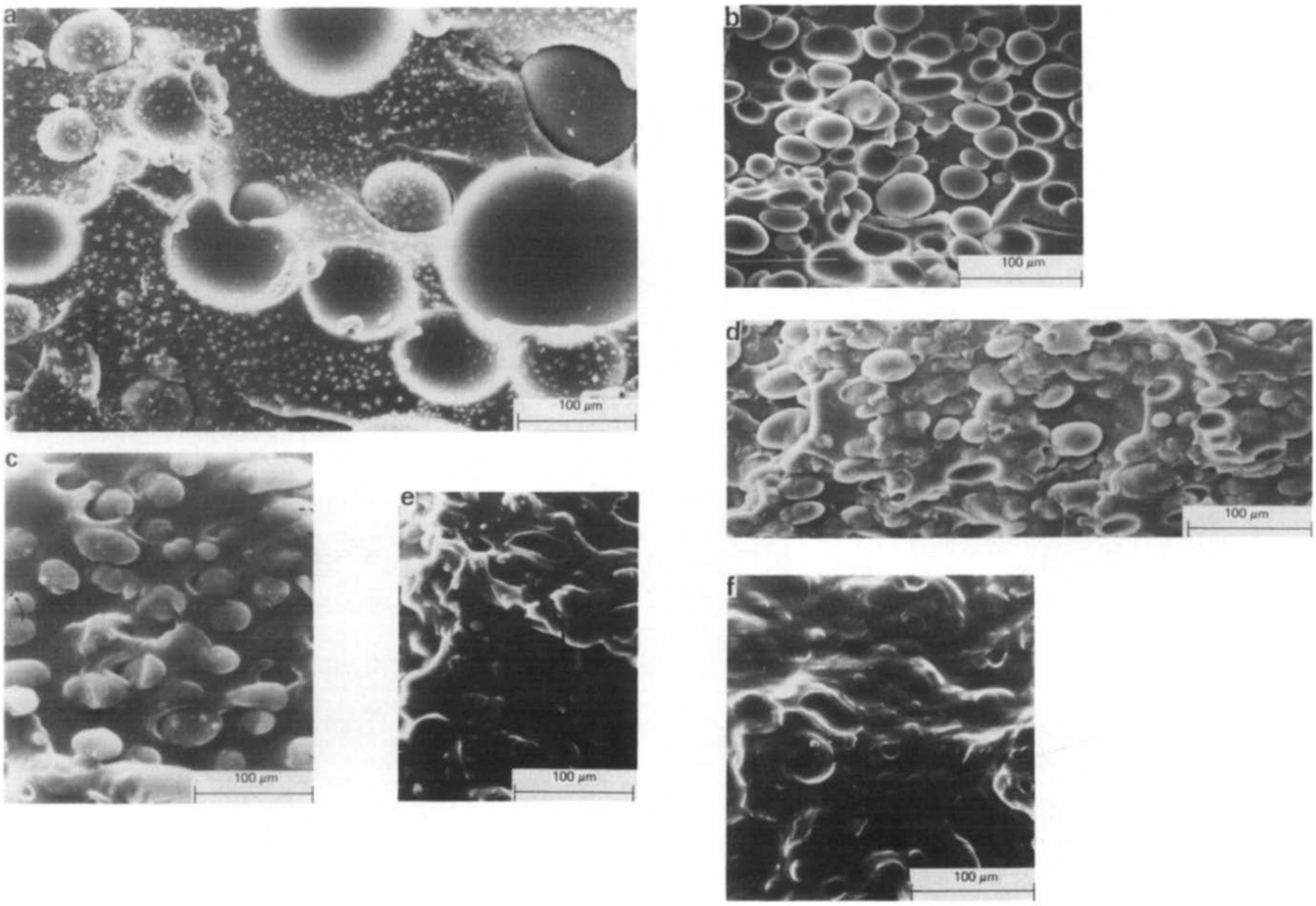

Figure 13 SEM micrographs of PUR–1000–30–595 modified blends: (a) no modifier; (b) 0.5%; (c) 1%; (d) 2%; (e) 5%; and (f) 10% modifier

line of *Table 6*. The size first decreases steeply with very small amounts (0.5%) of copolymer. Then the size decreases more slowly between 1% and 10% (limit of the study). It is interesting to note the good correlation between the morphology and mechanical behaviour of our blends. The best properties are obtained in the range 0.5–2% copolymer, with a maximum of the Young's modulus and elongation at break at 1%. In this case the nodules obtained are quite small and the adhesion seems to be good (see magnified scans in *Figure 14*). The better mechanical properties can be explained by both a diminution of the particle size and better interfacial adhesion, permitting an efficient transfer of stress between the matrix and the PDMS nodules. As discussed before, too much copolymer is harmful, and even if the particle size still decreases, the excess of copolymer acts like a plasticizer (the copolymer molecules are embedded in the polyurethane or PDMS network).

CONCLUSIONS

This study showed how it was possible to mix poly(urethane–ureas) and polydimethylsiloxane polydisperse networks. The blends obtained have very different morphologies before and after phase inversion. Between 10% and 40% PDMS in the blend, the polyurethane represents the matrix and the PDMS is dispersed in big non-adherent nodules (20–100 μm). On the other hand when the PDMS network forms the continuous phase, the polyurethane particle sizes are much smaller (0.3–1 μm). This can be explained by the differences of reactivity and viscosity observed between the two polymers. PUR and PDMS are so incompatible that the two phases observed are totally separate and the glass transition temperatures and ΔC_p of the soft phase of PUR are unchanged in all the blends. When the PDMS is in the continuous phase, T_g and ΔC_p are also constant, but when

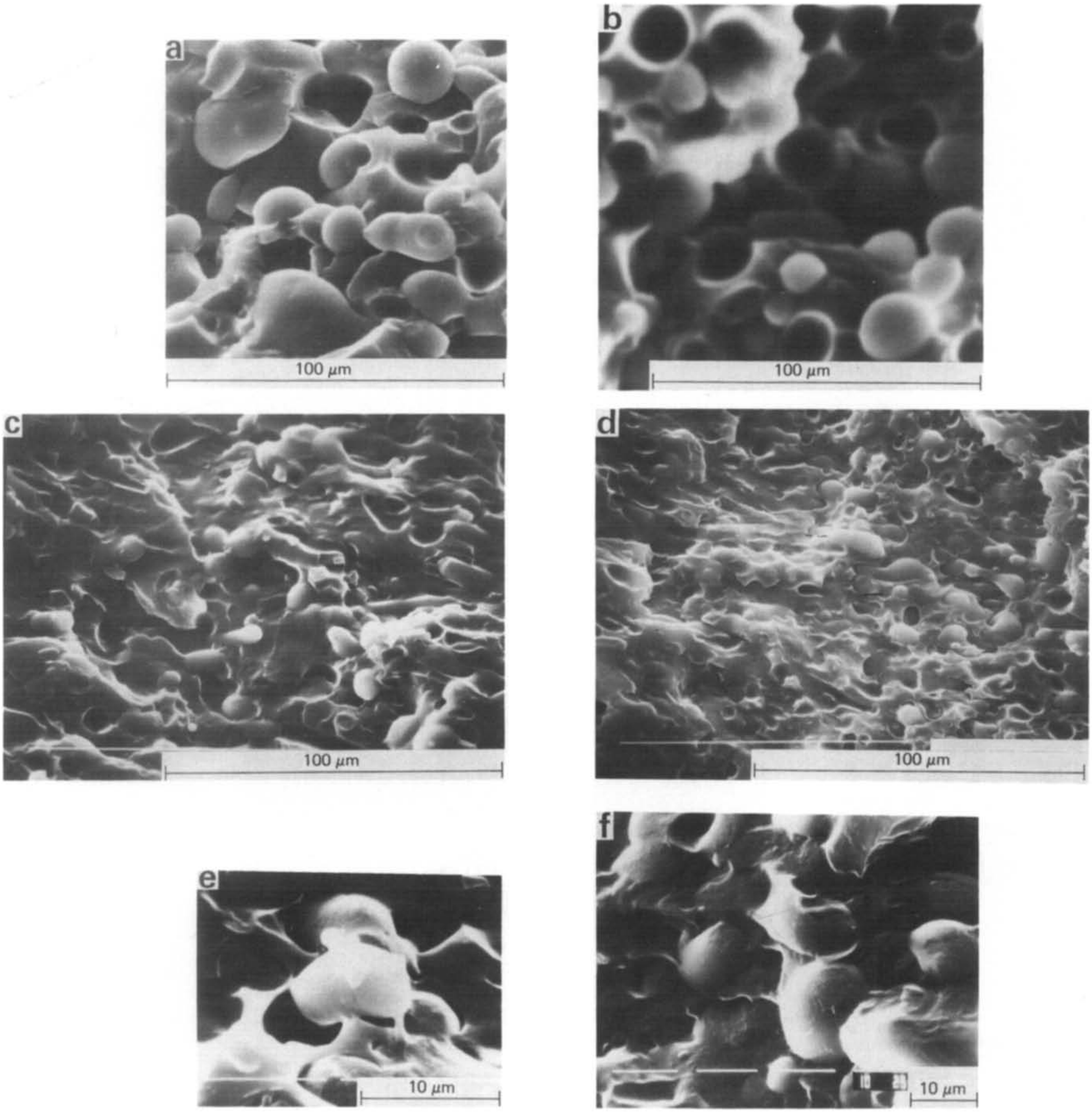

Figure 14 SEM micrographs of PUR 2000–30–595 blends (a) unmodified or modified with: (b) 0.5%; (c) 1% and (d) 2% copolymer. (e) and (f) are magnifications of (c) and (d) respectively

they are dispersed in nodules in a PUR matrix (between 10% and 40% PDMS), the glass transition is inexplicably displaced towards lower temperatures. This difference increases when the ratio of PDMS decreases, and can attain 6°C for a blend with 10% PDMS.

In the second part of the work, a PUR-*b*-PDMS block copolymer has been added to the blend to enhance the compatibility of the two polymers. The investigation of the morphology of the modified blends unambiguously supports the interfacial activity of the PUR-*b*-PDMS copolymer. The emulsifier is present at the interface, even though it is used in very small amounts (0.5–2%). As a consequence, the particle size is significantly reduced and the interfacial adhesion is enhanced. An excess of copolymer (more than 5–10%) is harmful. As a matter of fact the excess of copolymer in the PUR matrix acts like a plasticizer, so the mechanical properties of the blend are decreased. An interesting extension would be to optimize the synthesis of the copolymer and consider the enhancement of the interfacial adhesion *versus* the molecular weight of the two homopolymers.

ACKNOWLEDGEMENTS

Acknowledgement is made to the ALLRIM Society (Z.I. des Arbletiers, rue de la Jalesie, 25400 Audincourt, France) for financial support. We are grateful to Mrs Sylvie Garcon of the Dow Corning Corporation (France) for supplying PDMS liquid rubbers.

REFERENCES

1 Kempler, D., Frisch, H. L. and Frisch, K. C. *J. Elastoplast.* 1971, **3**, 2
2 Ebdon, J. R., Hourston, D. J. and Klein, P. G. *Polymer* 1984, **25**, 1633
3 Hourston, D. J., Huson, M. G. and McCluskey, J. A. *J. Appl. Polym. Sci.* 1986, **31**, 709
4 Hsu, T. T. and Lee, L. J. *Polym. Compos.* 1985, **25**, 951
5 Michaud, P., Camberlin, Y. and Maï, C. *Polym. Eng. Sci.*, in press
6 Sperling, L. H. 'Interpenetrating Polymer Networks and Related Materials', Plenum Press, New York, 1981
7 Arkles, B. and Peterson, W., 'Petrarch Systems Silicon Compounds', Petrarch, 2731 Bartram Rd, Bristol, PA 19007, USA
8 Barton, A. F. M., 'Handbook of Solubility Parameters and Other Cohesion Parameters', CRC Press, Boca Raton, 1983
9 Pascault, J. P. and Camberlin, Y. *Polym. Commun.* 1986, **27**, 230
10 Tyagi, D., Yilgor, I., McGrath, J. R. and Wilkes, G. L. *Polymer* 1984, **25**, 1807
11 Koberstein, J. T. and Stein, R. S. *Polym. Eng. Sci.* 1985, **24** (5), 293
12 Knaub, P. and Camberlin, Y. *J. Appl. Polym. Sci.* 1986, **32**, 5627
13 Fayt, R., Jérome, R. and Teyssié, Ph. *Makromol. Chem.* 1986, **187**, 837
14 Fayt, R., Jérome, R. and Teyssié, Ph. *J. Polym. Sci., Polym. Phys. Edn.* 1982, **20**, 2209
15 Rigby, D., Lin, J. L. and Roe, R. J. *Macromolecules* 1985, **18**, 2269
16 IKA Laboratory Technology, 'Technical Report'
17 Bellamy, L. J., 'The Infrared Spectra of Complex Molecules', 3rd Edn., Wiley, New York, 1975
18 Tesuka, Y., Tanaka, S. and Imaï, K. *Polym. Commun.* 1986, **26**, 327
19 Lemaitre, E., Thesis No. 331, 1983
20 Mark, J. E. *Makromol. Chem. Suppl.* 1979, **2**, 87
21 Falender, J. R., Yeh, G. S. Y. and Mark, J. E. *J. Chem. Phys.* 1979, **70** (11), 5324
22 Llorente, M. A., Andrady, A. L. and Mark, J. E. *J. Polym. Sci., Polym. Phys. Edn.* 1980, **18**, 2263
23 Lapp, A., Herz, J. and Strazielle, C. *Makromol. Chem.* 1985, **186**, 1919
24 Clarson-Dedgson, S. S. and Semlyen, J. A. *Polymer* 1985, **26**, 930
25 Flory, P. J., 'Principles of Polymer Chemistry', Cornell University Press, Ithaca, NY, 1953
26 Ferry, J. D., 'Viscoelastic Properties of Polymers', 3rd Edn., Wiley, New York, 1980
27 Flory, P. J. *J. Chem. Polym.* 1977, **66**, 5720
28 Graessley, W. W. *Adv. Polym. Sci.* 1974, **26**
29 Llorente, M. A. and Mark, J. E. *J. Chem. Phys.* 1979, **71** (2), 682
30 Llorente, M. A., Andrady, A. L. and Mark, J. E. *J. Polym. Sci., Polym. Phys. Edn.* 1981, **19**, 621
31 Chambon, F., Ph.D. Thesis, University of Massachusetts, 1986
32 Macosko, C. W., private communication
33 Flory, P. J. *Macromolecules* 1979, **12** (1), 119
34 Flory, P. J. and Takara, Y. I. *J. Polym. Sci., Polym. Phys. Edn.* 1975, **13**, 683
35 Muramoto, A. *Polymer* 1982, **23**, 1311
36 Flory, P. J. and Shih, H. *Macromolecules* 1972, **5**, 761
37 Barton, A. F. M., 'Handbook of Solubility Parameters and Other Cohesion Parameters', CRC Press, Boca Raton, 1983
38 Mooney, M. *J. Appl. Phys.* 1948, **19**, 434; Rivlin, R. S. *Phil. Trans. R. Soc. Lond. (A)* 1948, **241**, 379
39 Dagson, K. and Semlyen, J. A. *Polymer* 1977, **18**, 1265
40 Andrady, A. L., Llorente, M. A. and Mark, J. E. *J. Chem. Phys.* 1980, **72**, 2282
41 Valles, E. M. and Macosko, C. W. *Macromolecules* 1979, **12**, 673
42 Valles, E. M., Prost, E. J. and Macosko, C. W. *Rubber Chem. Technol.* 1983, **57**, 55
43 'Encyclopedia of Polymer Science and Technology', Interscience, New York, Vol. 12, 1970, pp. 464–569
44 Takayanagi, M., Harima, H. and Iwata, Y. *Mem. Fac. Eng. Kyushu Univ.* 1963, **23**, 1
45 Murayama, T., 'Dynamic Mechanical Analysis of Polymeric Material', Elsevier Scientific, Amsterdam, 1978, p. 64
46 Dickie, R. A. *J. Appl. Polym. Sci.* 1973, **17**, 45
47 Banderet, A., Tournut, C. and Reiss, G. *J. Polym. Sci. (C)* 1967, **16**, 2601
48 Jérome, R. and Fayt, R. *L'Actualité Chimique* 1980, **9**, 21
49 Lee, P. and McMaster, L. P. *Macromolecules* 1973, **6** (5), 760
50 Patterson, D. and Robard, A. *Macromolecules* 1978, **11** (4), 690
51 Cunliffe, A. K., Davis, A., Farey, M. and Wright, J. *Polymer* 1985, **26**, 301
52 Lorenz, O., Decker, H. and Rose, G. *Angew. Makromol. Chem.* 1984, **122**, 83
53 Knaub, P. and Camberlin, Y. *Eur. Polym. J.* 1986, **22** (8), 633